lubricants

MDPI

Article

Experimental Measurement of the Time-Based Development of Oil Film Thickness, Lubricating Film Extent and Lubricant Transport in Crosshead Engines

Graham Calderbank *, Edward H. Smith and Ian Sherrington

Jost Institute for Tribotechnology, School of Engineering, University of Central Lancashire, Preston PR1 2HE, UK; ehsmith@uclan.ac.uk (E.H.S.); isherrington@uclan.ac.uk (I.S.)
* Correspondence: gjcalderbank@uclan.ac.uk

Abstract: This paper describes the design of a test apparatus which simulates the lubrication of large, slow, two-stroke marine engines in which the ring pack is lubricated by means of injectors supplying lubricant above the piston. The equipment is able to control lubricant injection parameters (volume, frequency, etc.) and employs capacitance based lubricant film thickness transducers to allow instantaneous oil film thickness and film extent around the compression ring to be investigated on a stroke-by-stroke basis. It is demonstrated that the equipment can be used to study the development of lubricating films on successive strokes under differing injection strategies. Time varying changes in lubricating film thickness and film extent have been measured and the rate at which the lubricant spreads across the cylinder wall has also been investigated. It has been observed that increases in oil-film thickness are strongly linked to the transition from starved to fully-flooded inlet conditions and that net lubricant transport rates along different parts of the cylinder can be evaluated from measured data.

Keywords: piston ring-pack lubrication; oil film thickness measurement; IC engine lubrication

Citation: Calderbank, G.; Smith, E.H.; Sherrington, I. Experimental Measurement of the Time-Based Development of Oil Film Thickness, Lubricating Film Extent and Lubricant Transport in Crosshead Engines. *Lubricants* **2021**, *9*, 4. https://doi.org/10.3390/lubricants9010004

Received: 20 November 2020
Accepted: 23 December 2020
Published: 29 December 2020

1. Introduction

Large, slow, two-stroke, marine, diesel engines are typically used to power merchant vessels such as container ships and supertankers. These engines conventionally incorporate a crosshead, which serves two functions. The primary role is to isolate the combustion chamber's lubrication system from the lubrication of the rest of the crank-case, limiting the movement of corrosive combustion products and abrasive contaminants in the fuel to the rest of the engine and thus reducing damage to other engine components. The crosshead also supports the forces generated by the connecting rod in the direction normal to the cylinder liner, allowing for better lubrication and reduced friction and wear in the combustion chamber. The lubrication system for the piston-ring packs of modern, two-stroke, marine engines normally consists of some form of arrangement to spray lubricant into the cylinder at a position above the piston when the piston is in the lower part of the cylinder. The "swirl" of cylinder gases is sometimes used to assist in the distribution of the lubricant around the cylinder. In older systems, lubricant flows into the cylinder at a steady rate through a "quill" system consisting of a series of holes and channels in the cylinder with the passage of the ring pack helping to distribute the lubricant both axially and circumferentially. The majority of cylinder lubricant is burnt in the combustion process and across the global fleet the volumes involved are very large. Sherrington and Shorten [1] have estimated that over 1 m tonnes of cylinder lubricant per annum are consumed globally. It is believed that emissions from marine sources have a significant impact on the health of populations [2]. Thus, it is desirable to reduce the use of cylinder lubricants from both economic and environmental/health reasons.

In most two-stroke, marine engines, alkaline additives are supplied in the lubricant to neutralise acidic combustion products and thus reduce corrosion. The lubrication control system increases the lubricant supply-rate as engine speed or load increase, to allow a higher dosage of neutralizing additive as more acidic combustion products are generated. Consequently, more lubricant than that needed for lubrication purposes is commonly supplied to the cylinder.

Cylinder lubricant supply rates have gradually reduced over the last two decades, partly due to legislative requirements lowering the permitted proportion of sulphur-based content in fuel, but also because of significant economic pressure to lower lubrication costs. However, all commercial systems still rely on the link between lubricant supply rate and engine load/speed to administer the additive in the lubricant that neutralises potential corrosive substances. Over the last decade or so, this has led to serious corrosion problems, as ship engines have commonly been operated under unusual conditions of low load/speed conditions—called "slow steaming"—to increase fuel efficiency. This has been found to exacerbate a "cold corrosion" when ships docked and their engines are stopped [3]. Slow steaming is likely to remain in use for the foreseeable future as operators will need to meet efficiency and emission criteria [4]. The challenge of cylinder-lubricant supply has many facets and issues related to lubricant supply-rates are frequently discussed in literature [5].

Details of several simulation models of the lubrication mechanism of piston ring packs in marine engine have appeared only relatively recently in academic literature, for example [6,7]. These models are generally based on similar principles to those adopted when cyclic models of piston-ring lubrication in automotive applications were first developed in the early 1980s [8–10]. Unfortunately, models of lubrication in marine applications are more challenging to verify than those for automotive systems due to the operating cost and scale of marine engines. Tests have been conducted in bench test apparatus [11] and engine scale laboratory test equipment [12], but they do not fully replicate the true conditions of operating engines. However, some limited data is available. Moore [13,14] has measured lubricating oil film thickness on ship engines operating at sea. He identified a number of interesting features in this data including:

- Pre-lubrication of the cylinder, prior to start up, resulted in increased film thickness for up to 28 h in the top region of the stroke.
- There appeared to be correlation between Port and Starboard film thickness with one increasing as the other increased. In rough seas, this was seen to change with an increase in one side accompanied by a decrease on the other.
- Increases in feed rate appeared to lead to film thickness changes that took tens of minutes to stabilise while decreases in feed rate led to film thickness which fell much more quickly.
- Use of high viscosity grade lubricants seemed to result in slightly thinner films near TDC due to reduced transport capacity.
- Small changes in engine speed had an immediate and significant effect on film thickness.
- Abrupt vessel motion appeared to promote ring rotation.

Sherrington has proposed an alternative approach to cylinder lubrication which separates the two demands of lubrication and corrosion management [15]. The approach depends directly on feedback measurement of lubricating film thickness and cylinder acidity (pH) with lubricant and additives being supplied according to their individual demands at differential rates. This approach will potentially allow lubricant supply rates, and corresponding emissions to be significantly reduced, resulting in significant benefit to the environment as well as operational cost savings [1].

As a contribution to addressing this challenge, this paper presents an experimental investigation into how, on a stroke-by-stroke basis, lubricant is distributed throughout the cylinder of an engine by the action of a piston ring. This experimental study is also expected to guide improvements in fundamental calculations of the likely minimum required lubricant supply rate for marine engines which will require calculations of lubricant transport

rate (as well as calculations of lubricant consumption due to evaporation/burning). The observations made in this paper clearly suggest that changes in lubricating film thickness take place over modestly extended periods of time, and this is something that needs to be taken into account, in both practical lubrications systems and computer-based simulations of lubrication.

2. Materials and Methods

2.1. Experimental System

The experiments in this investigation were conducted on a motored, single-cylinder, Lister-Petter TR1 engine, modified to allow control of lubricant delivery to the cylinder above the piston. The absence of high cylinder pressures allowed the engine to be operated using a single piston-ring, simplifying the analysis for the theoretical model and improving comparability to the model. Key engine parameters are shown in Table 1.

Table 1. Lister-Petter TR1 Engine Specifications and Parameters for Experimental Work.

Scheme 98.	Value
Nominal cylinder bore	98.4 mm
Stroke	101.6 mm
Connecting rod length	164.0 mm
Cylinder capacity	773 cc
Compression Ratio	15.5:1
Minimum idling speed	850 rpm
Axial height of compression ring	2.75 mm
Radius of curvature of compression ring	30 mm
Rotational frequency of engine	120 rpm
Lubricating oil	20W-50 Mineral Oil

2.2. Lubricant Injection System

A spray lubrication system provided sufficient lubricant to ensure hydrodynamic lubrication of the piston-rings throughout the stroke. The volumetric flow-rate, lubricant injection frequency, and timing could all be varied.

Four Lincoln Industrial SL-43 metering injectors (SKF, Bedfordshire, UK), with delivery rates adjustable between 0.0164 mL and 0.131 mL per injection, connected to spray nozzles situated at the top of the cylinder, were employed. The injectors and spray nozzles were supported by a pneumatically operated injection circuit, including a solenoid for switching the air supply to the lubricant spray nozzles and the pneumatic pump that feeds oil to the metering injectors and spray nozzles (a schematic diagram of the circuit is shown in Figure 1). A microcontroller with a flywheel-mounted, hall-effect sensor was used to count engine revolutions and trigger lubricant injection at appropriate frequencies and crank angles. Figure 2 shows the spray nozzles mounted on the engine above the piston.

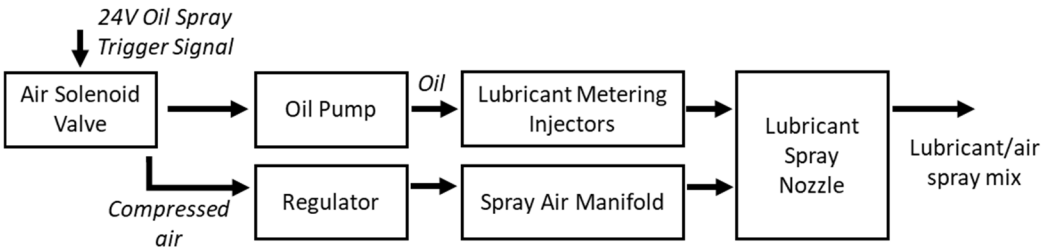

Figure 1. Schematic of the Spray Lubrication System.

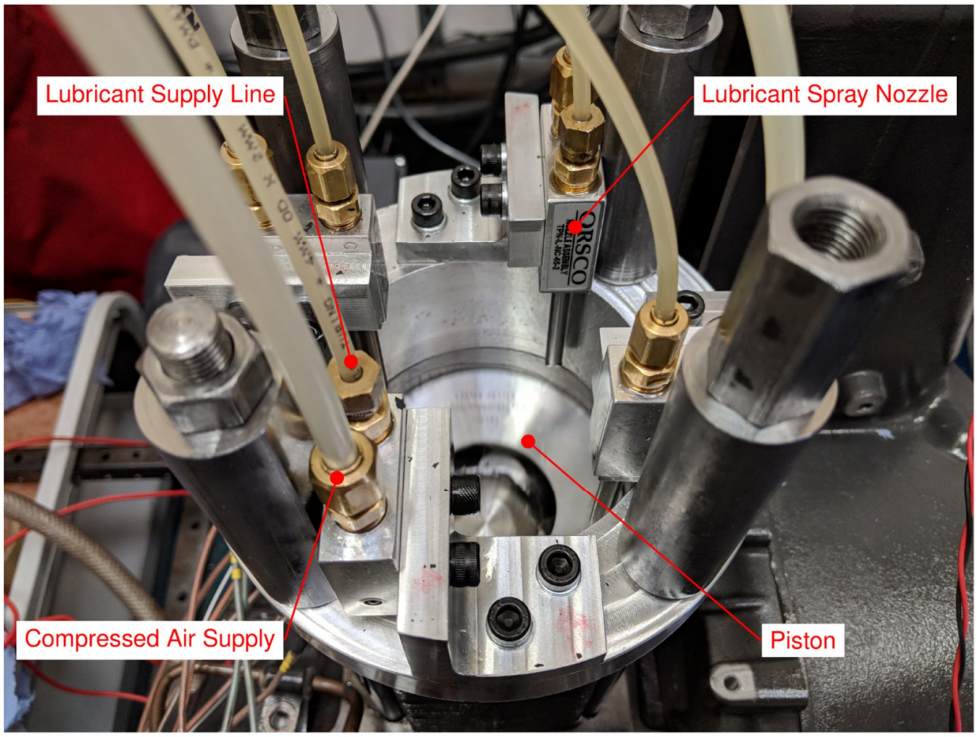

Figure 2. Cylinder head assembly with lubricant injectors fitted.

To determine the distribution of lubricant on the cylinder liner, lubricant was sprayed once onto a piece of paper inserted into the cylinder (the cylinder having been initially dry). The paper used had a height equal to the stroke length of the engine. A labelled image of the result of this test is shown in Figure 3. Image processing was used to highlight lubricant in yellow, with the dry cylinder coloured grey (other colours are artefacts of the image processing due to reflections and shadows from lighting). Figure 3 illustrates that the axial spread of the lubricant is from the near top-dead-centre to thr approximately 60–80 degrees crank angle. It is also evident that lubricant from the spray forms isolated "patches" which, in general, cover no more than 50% of the circumferential area in the top part of the cylinder. The oil at the bottom of the sample originated from absorption of excess lubricant between the cylinder liner and piston (which sat at bottom-dead-centre), it did not originate from the spray.

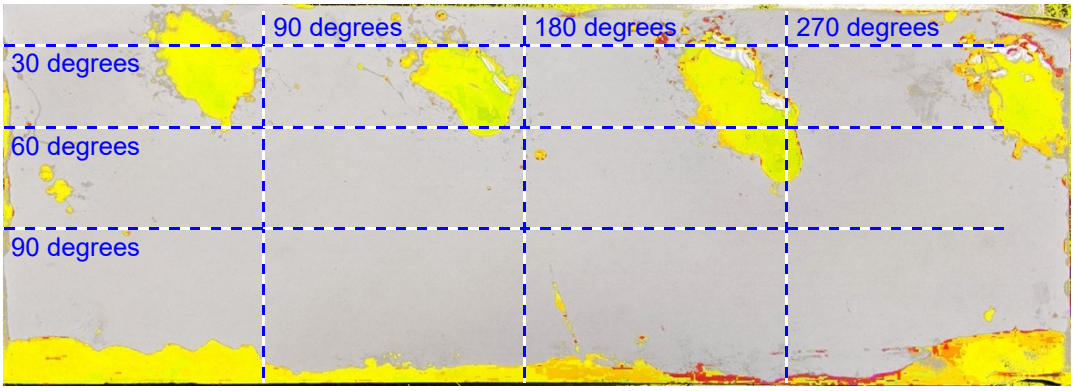

Figure 3. Sprayed lubricant distribution.

During investigations, lubricant could be sprayed from one or more injectors onto the top of cylinder at differing crank angles and differing frequencies (e.g., once per stoke, or

once in several strokes). Changing the position of the spray nozzle bracket also allowed the lubricant distribution on the cylinder to be adjusted.

2.3. Lubricant Selection

"Similarity" between the engine lubricating conditions during motored experiments and those when firing was desirable to acquire results which were representative of service conditions. To achieve this, Equation (1) was adopted. The ratio on the left-hand side of this equation was evaluated for the test engine during normal operating conditions near top dead centre on both power and induction strokes (giving values of 0.22 and 15), and for mid-stroke on the induction stroke (giving 60).

$$\frac{n_f U_f}{p_f} = \frac{n_e U_e}{p_e} \tag{1}$$

where η, U and p are dynamic viscosity, sliding velocity and contact load for the ring, with the sub-scripts f and e referring to the experimental and firing conditions. The experiments were conducted with no cylinder head fitted, so the pressure in the cylinder was atmospheric at all crank angles and consequently it was not possible to satisfy similarity under all test conditions. In order to ensure hydrodynamic lubrication over as much of the stroke as possible, a lubricant with a dynamic viscosity of 0.417 Pa.s was employed in order to satisfy the lower values of the similarity parameter.

The viscosity profiles of two lubricants were evaluated using an Anton Parr SVM-3000 Stabinger viscometer. Results from the tests suggested a 20W-50 lubricant as being most suitable for use in these experiments at typical room temperatures.

2.4. Surface Roughness Measurement

The use of specific film thickness, λ, defined as the ratio of oil-film thickness to the combined root mean square surface roughness of the interface surfaces, defined by Equation (2), is commonly used to determine the lubrication regime (i.e., boundary, mixed, hydrodynamic) in which a contact is operating [16,17].

$$\lambda = \frac{h_0}{\sqrt{R_{q1}^2 + R_{q2}^2}} \tag{2}$$

Surface profiles of both the barrel shaped compression ring, illustrated in Figure 4, and the cylinder liner were measured using a Taylor-Hobson Talysurf. The root mean square surface roughness averages, R_q, were evaluated for both, to allow the lower limit of full fluid-film lubrication to be estimated. The R_q of the piston-ring was 0.19 µm, and the R_q of the cylinder liner after honing was 0.55 µm. Using λ = 3 as the limiting value for hydrodynamic lubrication, the lower limit for fluid film lubrication was found to be 1.75 µm, thus allowing the contact regime to be established from the measured oil film thickness data.

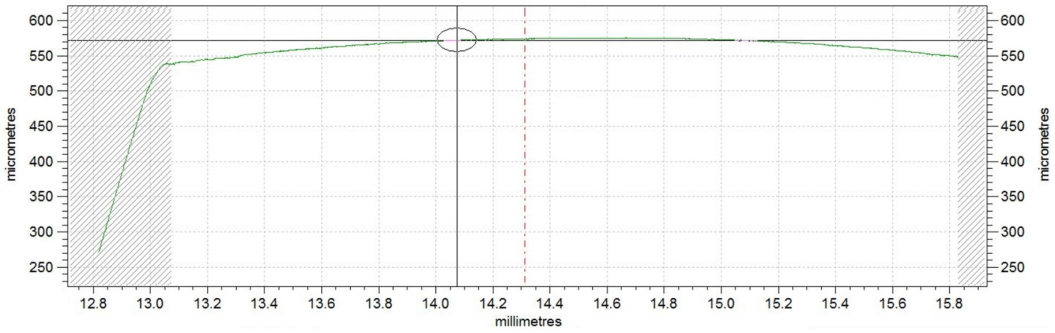

Figure 4. Surface profile of the top piston-ring. The right-hand land is not shown as the measurement aborts at this point due to the sudden change in height.

Capacitance oil-film thickness transducers were employed due to their reliability, accuracy, and ease of calibration. This type of sensor has extremely low noise, allowing accurate measurement of film thickness on a single pass. It has been successfully employed in both firing and motored engines to measure the lubricating film thickness. The absolute accuracy of film thickness measurement is influenced by a wide range of factors, but appears to be in the region of 8% across the measurement range with vertical resolution approaching 0.01 µm [18]. Lateral resolution is difficult to define and depends on the proximity of the ring to the transducer, but approaches the size of the transducer electrode (0.16 mm) at small film thickness. This is fine enough to determine the shape of piston-ring faces and identify machining marks on piston-rings [19]. Bespoke transducers were manufactured for this study. The maximum sampling rate of the transducer outputs was 10 kHz, which allowed around 30 data points to be captured as a ring passed at its highest speed.

2.5. Lubricant Film-Thickness Measurement

The equipment used was comparable to that employed by Garcia-Atance et al. [20]. The system uses parallel plate capacitor theory, for which the voltage output from the charge amplifier is given by Equation (3). Here, V_{osc} and C_{osc} are the oscillator input voltage and capacitance, ε_0 and ε_r are the absolute and relative permittivities of the lubricant, d is the distance between the electrode and the piston-ring, and A is the electrode area.

$$V_{out} = \frac{V_{osc} C_{osc} d}{\varepsilon_0 \varepsilon_r A} = k \frac{d}{A} \tag{3}$$

To locate the film thickness transducers, holes were drilled through the cylinder wall at strategic locations and the transducers secured with high performance adhesive. The cylinder was then honed. The low temperatures expected for motored experiments allowed a bespoke polymer tube to be used as an outer insulator. This material choice has an advantage over ceramic tubes more commonly used for high temperature devices, in that its roughness after honing closely resembles that of the cylinder itself. The polymer tube was produced using stereo lithographic 3D printing, the resin used being Formlabs Grey, which had an elastic modulus of 2.8 GPa.

Transducers were positioned to investigate the effects of lubricant flow-rate and distribution on oil-film thickness (see Figure 5). Since lubricant was delivered from four injectors, a variable distribution of transducers was adopted around the circumference of the cylinder liner. They were positioned axially along a line through the centre of one of the lubricant spray delivery zones to capture the region with the greatest volume of lubricant (block II), with another line of transducers positioned in the intersecting region to capture oil-film thickness where lubricant volume was minimal (block I). Three further sensors (blocks III–V) were located around the circumference of the cylinder liner at an axial location 31 mm below top dead centre (correspondent with a crank angle of 60° from top dead centre) to allow investigation of circumferential lubricant flow.

Lubricant film thickness channels on two amplifiers were calibrated to establish the relationship between voltage output and lubricant film thickness for the lubricant used for the investigations (20W-50 mineral oil.).

The transducers were installed slightly proud of the surface and subsequent honing of the cylinder aligned the cylinder and transducer surfaces and provided them with a similar surface finishes to provide a continuous surface for lubrication. Due to the mixture of materials used, this process was not perfect and slightly different material removal rates were evident on the cylinder and the differing transducer components (see Figure 6). Since the transducers are small and rather few, we anticipated that any imperfections on the transducer surface will have a negligible effect on the overall lubrication of the piston ring. Surface replicas at each sensor location in the cylinder were obtained in order to accurately determine the average position of the transducer surface with respect to the average roughness of the liner surface. This allowed post-processing of the data to give

accurate readings for oil-film thickness as a distance from the cylinder surface rather than the potentially fractionally different distance from the ring to the transducer electrode. Each replica was scanned using a MicroXAM 10000 white-light interferometer (ADE Phase Shift, Tucson, AZ, USA) to determine the surface height across a section of the sensor. The replica was carefully aligned in the axial direction in order to minimise height changes due to its curvature, and the table upon which it sat was adjusted such that the replica was horizontal. To determine the offset between the cylinder liner and the electrode, the mean surface height was taken on each side of the transducer, as well as the surface height at the electrode. An example of one of these replicas is shown in Figure 6.

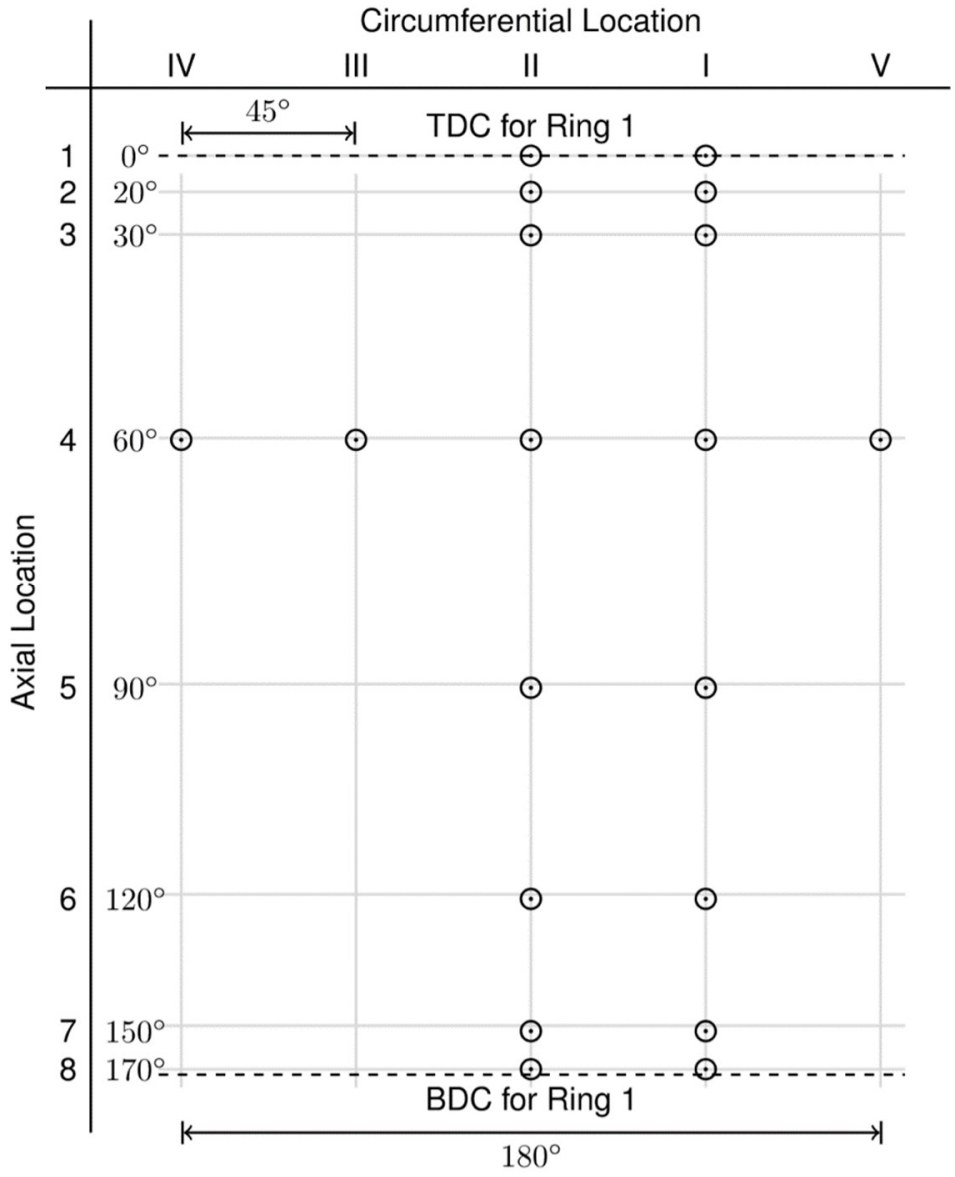

Figure 5. Sensor positions and reference grid on the 'unwrapped' cylinder wall.

In addition to the above calibration, installed transducers were inspected to ensure the honing process had not produced excessive smearing of the electrode, this effect can influence the transducer output and hence oil-film thickness results. Inspection showed that smearing was minimal, and no corrections to the oil-film thickness were applied for this effect.

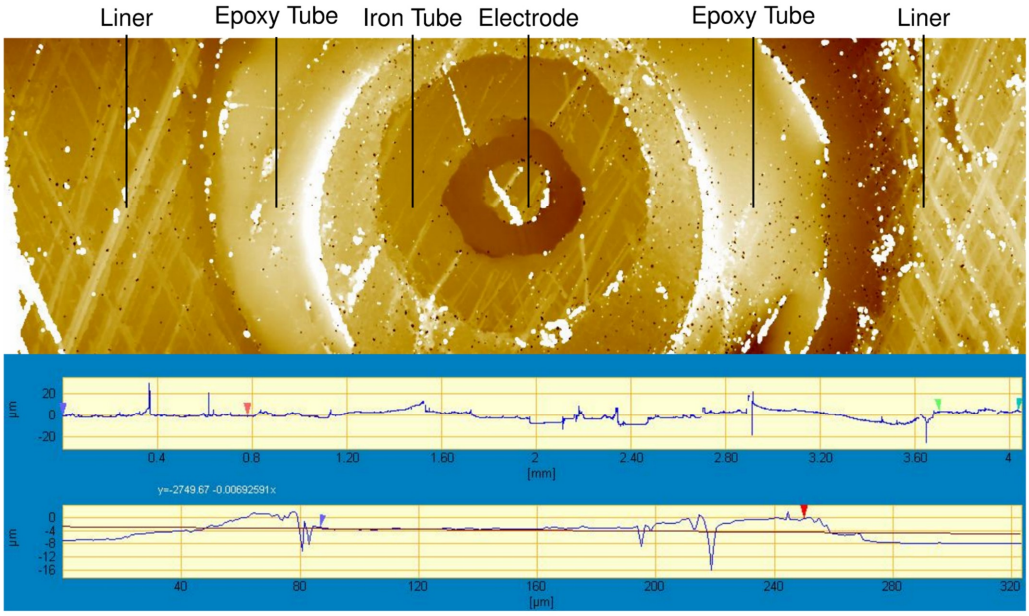

Figure 6. White light interferometer scan of sensor I-1, with axial (**top**) and circumferential (**bottom**) sections through the electrode.

2.6. Preliminary Results

The output signals from the transducer amplifiers were found to have very low noise. A typical, unfiltered measurement from a single ring pass is illustrated in Figure 7. (Sensor II-4, located 31 mm below Top Dead Centre (TDC)). The solid line is the measurement signal from the sensor, and the dotted line the estimated shape of the ring based on a predicted signal (using Equation (3)). The estimated shape was evaluated by convolving the real shape of the piston-ring (determined using a Talysurf contour measurement of the ring-face profile taken before the experiment), the measured minimum oil-film thickness from the experiment, and the shape of the circular transducer electrode. This is necessary, especially when the ring does not fully overlap with the electrode, because the geometry of the arrangement influences the capacitance (and therefore, the apparent lubricating film thickness measured) by the transducer (In this case the simulation assumes the contact is fully-flooded with lubricant). The process for conducting this calculation is non-trivial and described elsewhere [20]. The difference in Figure 7a between the two curves is due to cavitation in the outlet region of the ring. Here the measured signal deviates from the simulated signal due to the reduction in relative permittivity where air is present between piston-ring and the cylinder. Both cavitation and starvation are present in Figure 7b, where the output from sensor I-4 is presented.

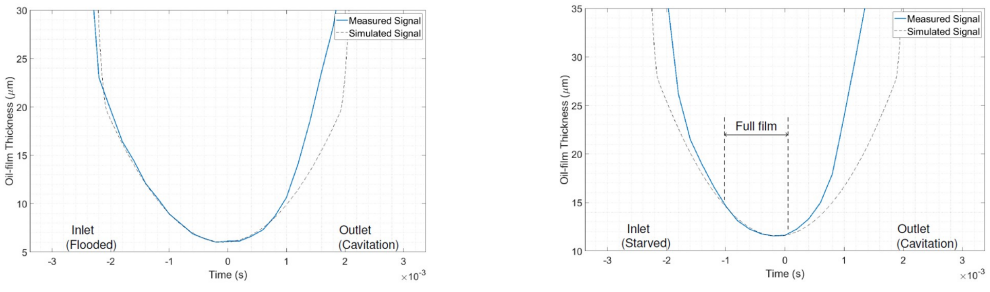

(**a**) (**b**)

Figure 7. Measured vs simulated signals with spatial coordinates on the horizontal axis: (**a**) Sensor II-4, flooded inlet; (**b**) Sensor I-4, starved inlet.

3. Results

Experiments were conducted to examine the effect of localised lubricant delivery on oil-film thickness and lubricant transport.

The tests were performed at four lubricant injector flow-rates; 0.01 millilitres per injection (mL inj^{-1}), 0.02 mL inj^{-1}, 0.04 mL inj^{-1}, and 0.08 mL inj^{-1}. On each cycle, lubricant was injected onto the cylinder liner in 4 locations, shown in Figure 8. Only the compression ring was employed in these tests. The oil-film thickness for this piston-ring was measured on every stroke of each 30 second test.

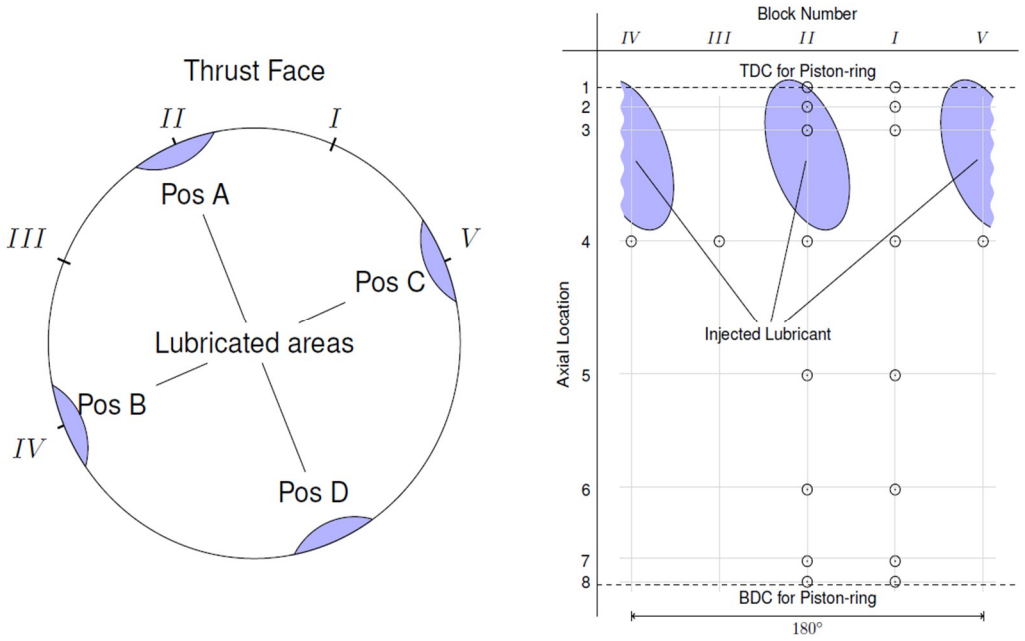

Figure 8. Location of lubricant and transducers in the cylinder.

Lubricant injector valves were open for 200 ms on every cycle, commencing when the piston ring was moving downwards at 82 mm below top dead centre. One of the spray lubricated areas was aligned with the first three sensors in block II (top dead centre to 31 mm below top dead centre), while three additional lubricated areas was equally spaced in a circular pattern about the cylinder axis. Engine and experimental parameters for this experiment are detailed in Table 1. The cylinder liner was cleaned thoroughly with solvent after each test to ensure no residual lubricant was present at the start of each run.

3.1. Time Based Variation of Lubricating Film Thickness

Film thickness was found to change with time as illustrated in Figure 9, where film thickness data for four different supply rates are plotted for sensor II-4. Film thicknesses oscillated considerably for the first 20 cycles. After the 35th cycle, reasonably constant film thicknesses were obtained.

Oil film thickness measurements for four transducers in Block I and four transducers in Block II are given in Figures 10 and 11, for two different injection rates. Here the time scale for each data set was 30 s, corresponding to 60 reciprocating cycles. Transducers I-3 and I-4 in Block II (Figure 10), which were closer to the initial deposit of sprayed lubricant quickly developed significant hydrodynamic films and these stabilised at reasonably constant values after a few seconds. Further away from the initial deposits (sensors 5 and 6), it took longer for the oil to be transported to the sensors and thus much lower film thicknesses were initially obtained. Erratic behaviour was exhibited in the outputs of these two sensors due to surface contact. After some delay, lubricant flowed to these sensors, and reasonably stable films were formed. Figure 11 presents outputs from four transducers in Block II. It

would be expected that film thicknesses here would be greater than in Block I because the original oil deposits lay directly over the upper transducers in this block. That this was not the case is still not clearly understood. Despite this, the outputs (for example at II-4 and II-5) show less of the erratic behaviour and the increases in oil-film thickness begin, and plateau, earlier in the test. This suggests less contact between piston-ring and cylinder and that lubricant is being transported more quickly to these transducers.

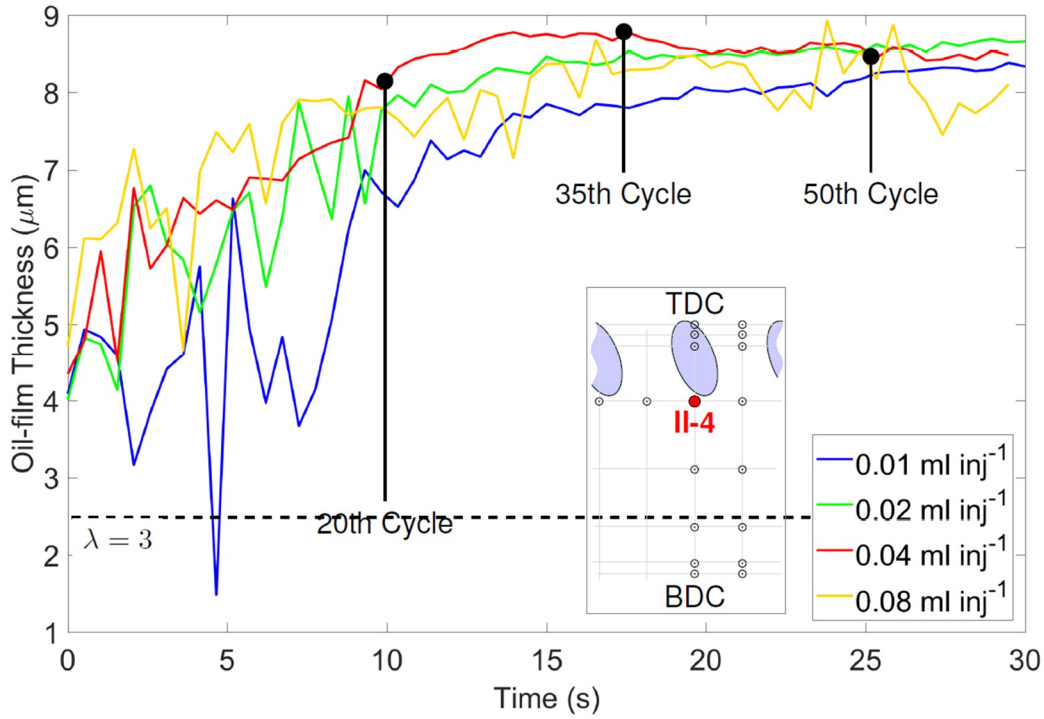

Figure 9. Minimum oil-film thickness on upstrokes at sensor II-4 during tests at four lubricant injector flow-rates.

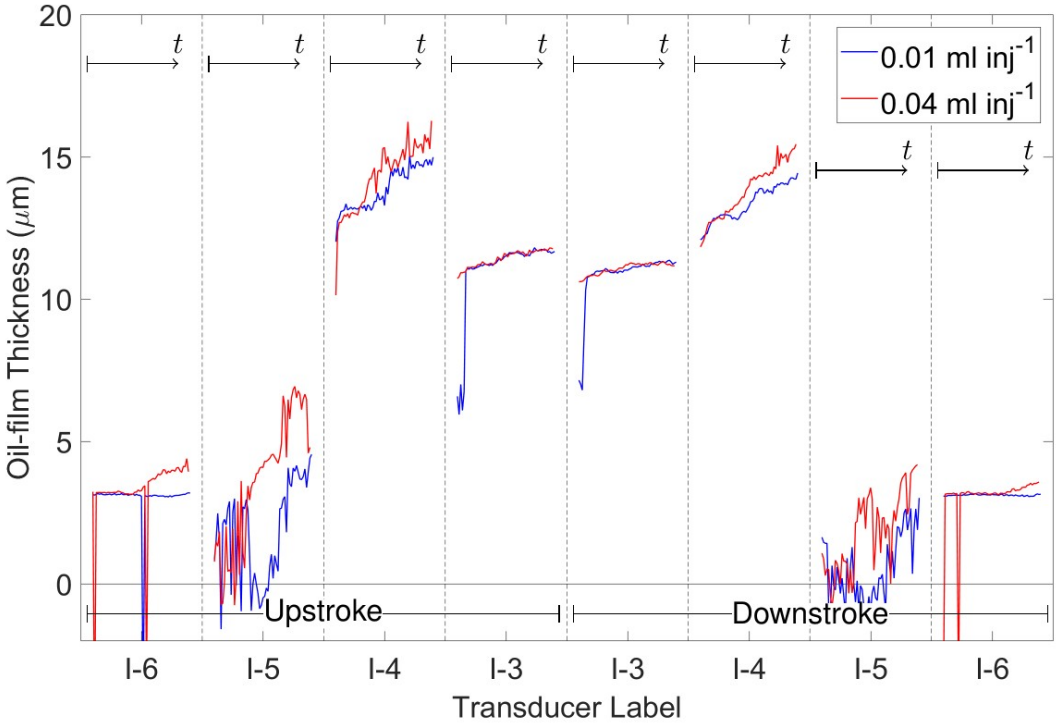

Figure 10. Graphs of minimum oil-film thickness vs. time at sensors I-3 to I-6 Block I.

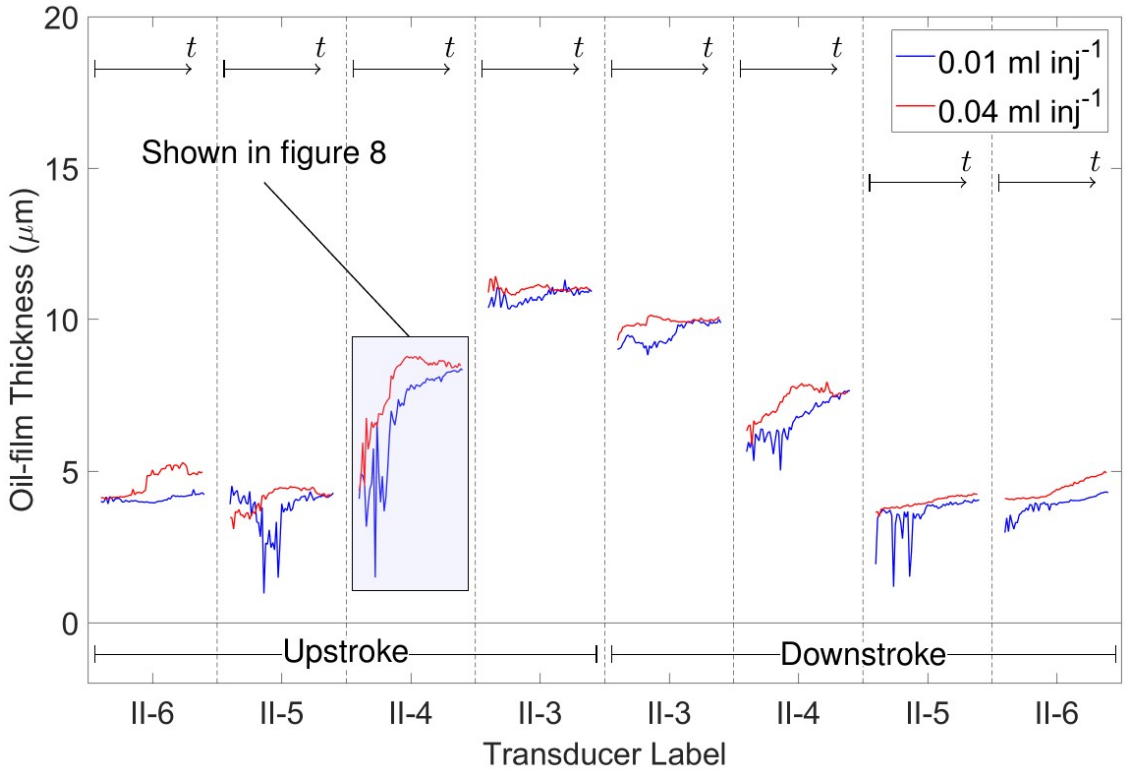

Figure 11. Graphs of minimum oil-film thickness vs. time at sensors II-3 to II-6 Block II.

3.2. Time Based Variation in Lubricating Film Extent

The degree of filling (film extent) across the width of the piston ring was also assessed as a function of time (number of strokes) and results are presented in Figure 12 for an injection rate of 0.01 mL inj^{-1}. The abscissae of these charts are the axial coordinates of the ring, and the ordinate is time (with 0 s at the upper right part of each graph). It can be seen that more flooded inlet conditions tend to develop at the sensors nearest to the lubrication point first, with those lower down the cylinder being more extensively lubricated as lubricant arrives after a greater number of strokes. Interestingly, the full film extent appears to develop rather abruptly, rather than gradually at each sensor location.

In most cases, the film extents showed the piston-ring to be highly starved at the beginning of the tests, with the inlet boundary moving towards the piston-ring inlet over time. Transducer II-3 is the exception, but this is to be expected, as lubricant is sprayed onto this part of the cylinder. This transition from starved to fully flooded occurs earlier for transducers near the top dead-centre. As the lubricant film develops oil is scraped further down the cylinder on each cycle until it reaches these transducers.

The increases in film-extent for sensors in block II also occurred earlier than seen for block I. With the lubricant being delivered near the top of block II, it appears that oil is transported axially more quickly than it is circumferentially.

There is an apparent link between the timing of the (near) step-changes in oil-film thickness increases and film-extent, particularly for transducers 4 and 5. For example, transducer II-4 showed an increase in both film thickness and extent at approximately 10 s (20 cycles), while transducer I-4 showed a similar change at 15 s (30 cycles).

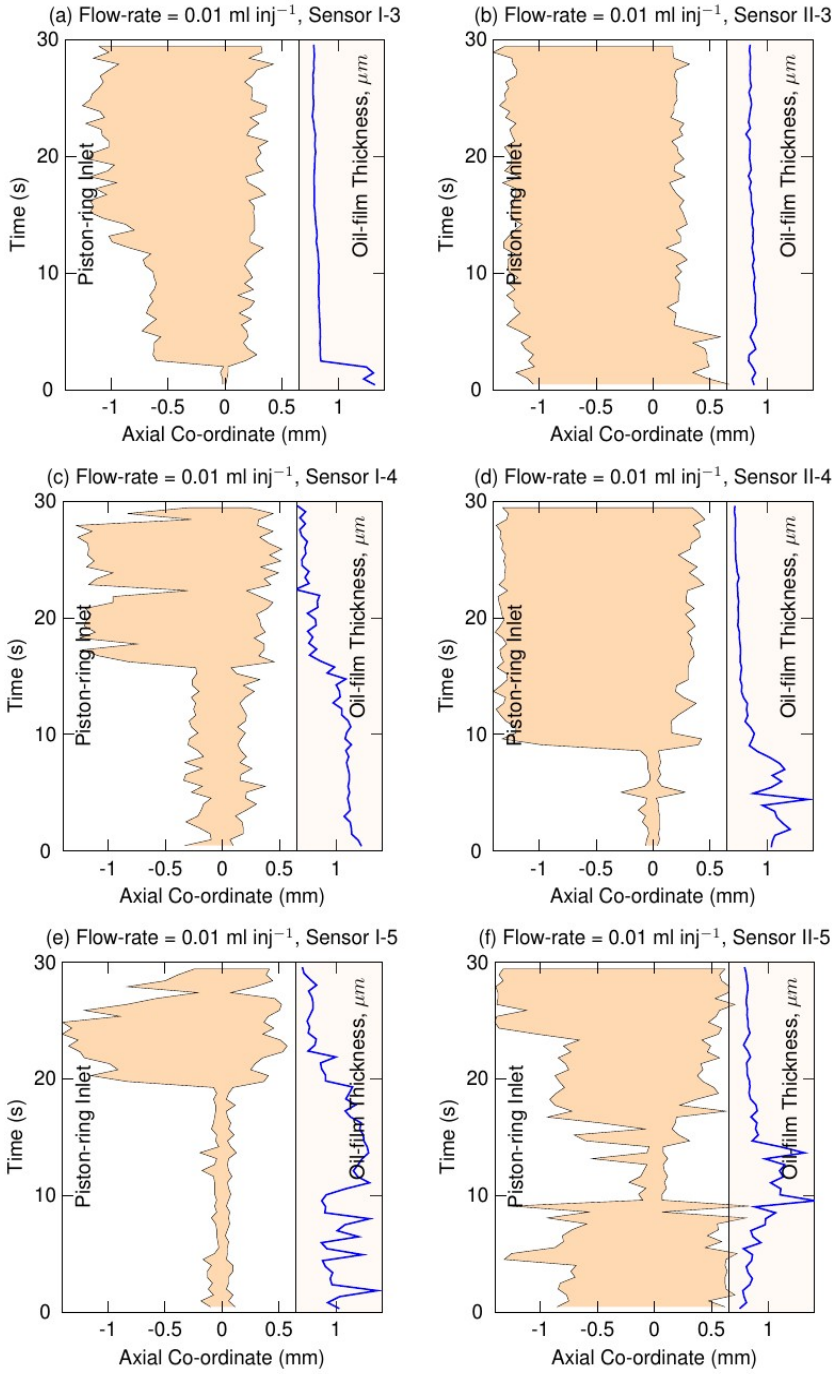

Figure 12. Experimental inlet and cavitation boundaries taken on the upstrokes.

4. Discussion

Developing a method to evaluate in-cylinder lubricant transport rates has long challenged engine tribologists. Early investigators used optical access to gain a qualitative understanding of the position of lubricant volumes at different parts of the stroke in motored engine cylinders [21,22]. Techniques to study lubricant flow to various parts of the piston-assembly using laser induced fluorescence (LIF) and dyes to enhance the visibility and movement of lubricant, have also been used, mainly in motored engines [23,24]. Lubricant degradation analysis has also been used to estimate flow rates from the sump to the ring pack [25] and for lubricant return cycles through the ring pack and back to the sump [26]. Various methods have also been developed to accurately evaluate flow entire through the cylinder in the form of lubricant consumption. One example of this involves

using real-time measurement of sulphur dioxide tracers [27]. However, a reliable method to quantitively evaluate flow rate of lubricant moving between different points within the cylinder due to the various transport mechanisms operating within the ring pack has proved more challenging.

The configuration of this test apparatus permits the implementation of a technique to measure the change in volume of lubricant between piston-ring and cylinder liner at a given location within the cylinder on a stroke-by-stroke basis. This volume is evaluated using film-thickness and film extent data from oil-film thickness sensors on each cycle. When these data are monitored during a transient phase in lubricating film conditions, for example during a test (such as those discussed here) from an initially (unlubricated) dry cylinder, or following a change in engine conditions/lubricant flow rate, the volume changes measured at a series of sensors positioned axially along the cylinder liner allow the lubricant transport to be computed.

Evaluating lubricant transport involves dividing the cylinder wall into a number of control volumes that extend around the full circumference of the cylinder, as illustrated in Figure 13. Each volume surrounds one of the sensors. It is assumed that the volume of oil contained within the full fluid film at a specific sensor remains constant as the ring passes from the upper edge of the control volume to its lower counterpart.

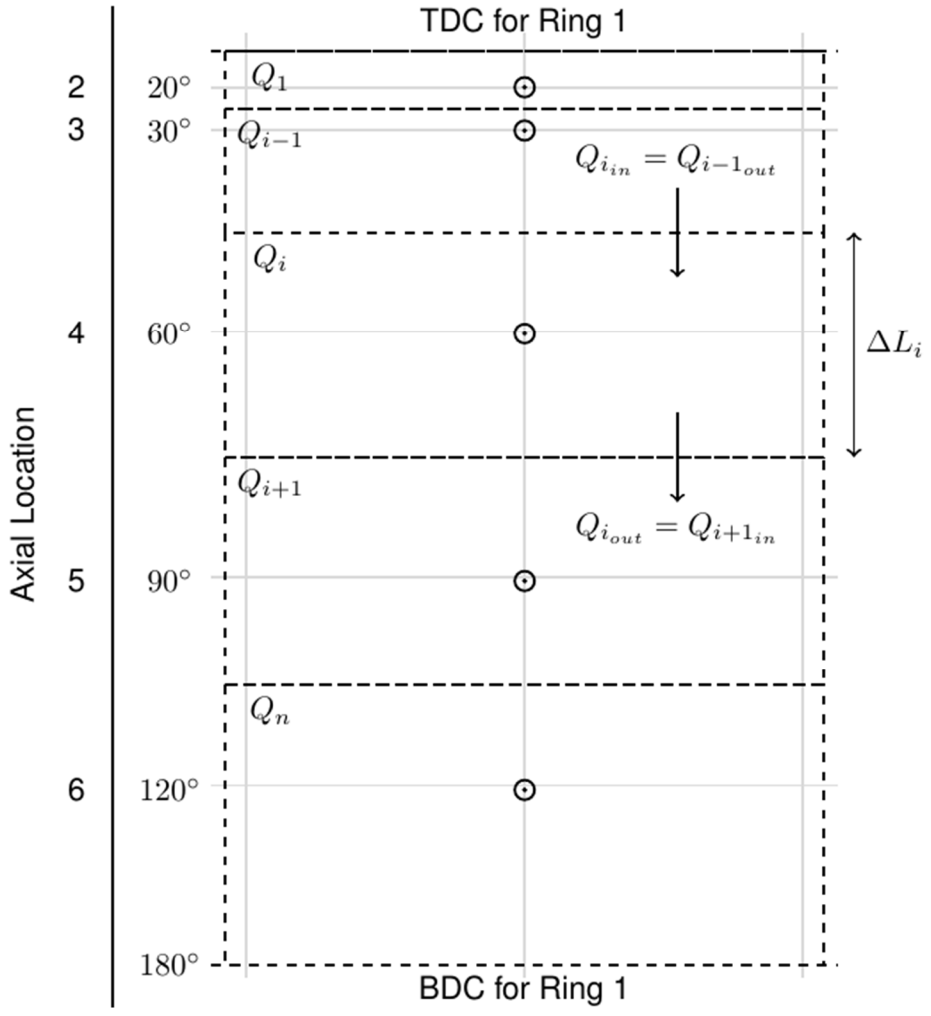

Figure 13. Boundaries (dashed lines) along the cylinder for integration zones.

It is possible to use the Couette flow to estimate the lubricant flow volume. This is achieved by assuming that the minimum film thickness (h_0) occurs close to the maximum pressure, so the thickness of the lubricant film left on the cylinder wall, after the ring has

passed, is approximately half the minimum film thickness. Consequently, the lubricant flow volume (shown in Figure 14), or the volume of oil remaining on the cylinder wall at the end of the stroke can also be estimated by integrating half the minimum film thickness over all the control volumes (Equation (4)).

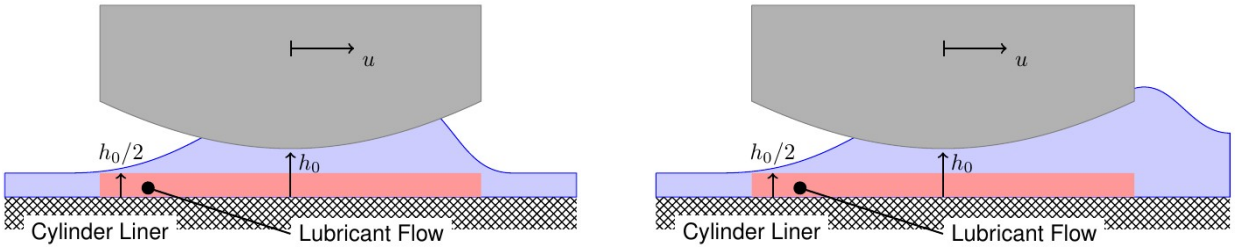

(**a**) (**b**)

Figure 14. Schematic showing both the calculated lubricant volume from the integration method using oil-film thickness and film extent and the calculated lubricant flow for a piston-ring with: (**a**) Starved inlet; (**b**) Fully-flooded inlet.

$$\sum_{1}^{n} V_i = \frac{\pi D}{2} \sum_{1}^{n} \Delta L_i (h_0)_i \tag{4}$$

The net lubricant transport can be estimated by determining the differences between the values calculated from Equation (4) on the down and up strokes. Figure 15 shows an example of the results obtained for the experiment described where the cylinder was initially dry, and lubricant was sprayed onto the cylinder liner on every cycle. The figure shows summed volumes from the lubricant flow volume calculation (Equation (4)), for upstrokes and downstrokes. Also shown on the graph is the net lubricant transport downwards.

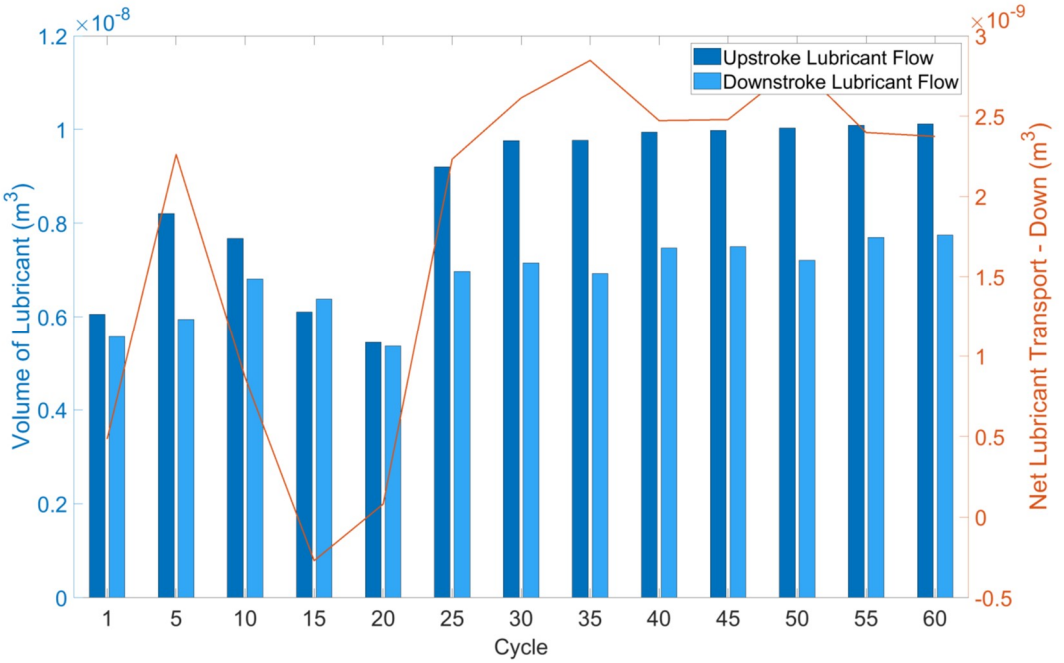

Figure 15. Total lubricant flow and net transport downwards over of the number of strokes.

Lubricant volumes generally show higher quantities left behind on the upstrokes than the downstrokes, indicating there is a net downflow of fluid. In the early part of the test, when the piston-ring is highly starved, there is little change in the thicknesses of the films

left on the cylinder wall, but as the lubricant film develops, a small amount is transported down the cylinder to bottom dead centre on each cycle.

Figure 15 shows also the net lubricant transport to reach a near constant value from cycle 30 onwards. Lubricant is initially concentrated near to where the lubricant is sprayed onto the cylinder liner (the top third of the stroke). As the test progresses, the downwards transport of oil leads to the lubricant film progressively extending further towards the bottom dead centre. After 30 cycles, it appears that the lubricant film is sufficiently developed over the entire stroke as to have reached a steady state, where any further lubricant sprayed onto the cylinder liner is scraped away to the bottom dead centre. In the later cycles, the inlets are almost flooded (see Figure 12) and, indeed may be flooded, resulting in some upward scraping of oil that is then deposited in the top dead centre region. This may explain why the net lubricant transport is less than that supplied (1×10^{-8} m^3 inj^{-1} or 0.01 mL inj^{-1}).

5. Conclusions

A test apparatus has been designed and commissioned in which a single piston ring reciprocates in the cylinder of a small diesel engine. Lubricant was sprayed on to the cylinder wall from a set of injectors, and a range of flow rates and injection frequencies, have been studied. A number of capacitance transducers were installed and the lubricant film thickness measured as the ring passed each sensor. Changes in film extent have also been examined at the same locations and over the same time period. Increases in oil-film thickness appear to be strongly linked to increases in film extent.

It has been possible to estimate the transport of lubricant by estimating the thickness of lubricant films left on the cylinder wall as the ring passes over it. It is found that the films are thicker after an upstroke than a downstroke, suggesting that there is scraping of oil down the cylinder. There is also a suggestion that some excess oil is scraped upwards in the later cycles and deposited at the top dead centre location.

A strong trend exists in industries using internal combustion engines for power to shift towards electrification and hybridisation, including within the maritime shipping industry in order to meet the IMO's target of cutting annual emissions in maritime shipping by 2050 to 50% of 2008 levels [28]. Despite this, the long life of shipping vessels leads to relatively low turnover of new power units relative to, for example, the automotive industry, and it is expected that internal combustion engines will remain in use for many years yet. As such the development of systems such as those proposed to better control piston-ring lubrication for reduced wear, lower emissions, and reduced cylinder oil consumption will be key to meeting current and future legislation. Systems such as this will be heavily reliant on developing techniques for the real-time monitoring of oil-film thickness and other aspects of the lubrication conditions.

Author Contributions: Conceptualization, G.C., E.H.S. and I.S.; Formal analysis, G.C., E.H.S. and I.S.; Investigation, G.C.; Methodology, G.C.; Supervision, E.H.S. and I.S.; Visualization, G.C.; Writing—original draft, G.C.; Writing—review & editing, E.H.S. and I.S. All authors have read and agreed to the published version of the manuscript.

Funding: This research received no external funding.

Institutional Review Board Statement: Not applicable.

Informed Consent Statement: Not applicable.

Data Availability Statement: Publicly available datasets were analyzed in this study. This data can be found here: [http://clok.uclan.ac.uk/36203/1/OFTData.zip].

Conflicts of Interest: The authors declare no conflict of interest.

Abbreviations

The following abbreviations are used in this manuscript:

A	Electrode area
C	Capacitance
d	Electrode diameter
D	Cylinder bore
h_0	Minimum oil-film thickness
L	Control volume length
p	Combustion chamber pressure
Q	Lubricant volume
R_q	Root-mean-square roughness
U	Piston speed
V	Voltage

Greek Letters

ε	Permittivity
λ	Specific film thickness
η	Dynamic viscosity

References

1. Sherrington, I.; Shorten, D. Influences on the Lubrication of Piston-Rings in Large Two Stroke Diesel Engines and the Impact of MARPOL VI. In *Proceedings of LUBMAT 2006, Preston, UK, 14–16 June 2006*; Sherrington, I., Velasco, F., Arnell, D.A., Smith, E.H., Sperring, T., Eds.; University of Central Lancashire: Preston, UK, 2007; ISBN 978-1-901922-64-6.
2. Corbett, J.J.; Winebrake, J.J.; Green, E.H.; Kasibhatla, P.; Eyring, V.; Lauer, A. Mortality from ship emissions: A global assessment. *Environ. Sci. Technol.* **2007**, *41*, 8512–8518. [CrossRef] [PubMed]
3. CIMAC Working Group 8 Marine Lubricants. Cold Corrosion in Marine Two Stroke Engines. In *CIMAC Guideline*, 1st ed.; CIMAC: Frankfurt, Germany, 2017.
4. The Motorship: Insight for Marine Technology Professionals. 2020. Available online: https://www.motorship.com/news101/fuels-and-oils/200bn-marine-cylinder-lubricant,-a-new-solution-for-engines-running-on-hsfo (accessed on 13 December 2020).
5. Canter, N. Marine diesel cylinder engine oils: Lubrication challenges impacted by operating conditions and regulations. *Tribol. Lubr. Technol.* **2017**, *73*, 10–21.
6. Wolff, A. Influence of Engine Load on Piston Ring Pack Operation of a Marine Two-stroke Engine. *J. KONES Powertrain Transp.* **2012**, *19*, 557–568. [CrossRef]
7. Overgaard, H.; Klit, P.; Vølund, A. Investigation of different piston ring curvatures on lubricant transport along cylinder liner in large two-stroke marine diesel engines. *Proc. Inst. Mech. E Part. J J. Eng. Tribol.* **2017**, *232*, 85–93. [CrossRef]
8. Ting, L.L.; Mayer, J.E., Jr. Piston Ring Lubrication and Cylinder Bore Wear Analysis, Part I—Theory. *ASME J. Lubr. Tech.* **1974**, *96*, 305–313. [CrossRef]
9. Ting, L.L.; Mayer, J.E., Jr. Piston Ring Lubrication and Cylinder Bore Wear Analyses, Part II–Theory Verification. *ASME J. Lubr. Tech.* **1974**, *96*, 258–266. [CrossRef]
10. Ruddy, B.; Economou, P.N.; Dowson, D. The Theoretical Analysis of Piston Ring Performance and its Use in Practical Ring Pack Design. In Proceedings of the 14th International Congress on Combustion Engines, Helsinki, Finland, 6–11 June 1981.
11. Li, T.; Ma, X.; Lu, X.; Wang, C.; Jiao, B.; Xu, H.; Zou, D. Lubrication Analysis for the Piston Ring of a Two-stroke Marine Diesel Engine Taking Account of the Oil Supply. *Int. J. Engine Res.* **2019**. [CrossRef]
12. Klit, P.; Vølund, A. Experimental Piston Ring Tribology for Marine Diesel Engines. In Proceedings of the STLE/ASME 2008 International Joint Tribology Conference, STLE/ASME 2008 International Joint Tribology Conference, Miami, FL, USA, 20–22 October 2008; pp. 493–497.
13. Moore, S. The Influence of Engine Operating Parameters on Piston-ring Oil Film Thickness in a Marine Diesel Engine. In Proceedings of the CIMAC Congress, Interlaken, Switzerland, 15–18 May 1995.
14. Moore, S. The Complexities of Piston-ring Oil Lubrication in a Large Two Stroke Marine Diesel Engine. In Proceedings of the CIMAC Congress, Copenhagen, Danemark, 18–21 May 1998; pp. 575–586.
15. Sherrington, I. Lubrication Control System. GB Patent 2,357,556, 27 June 2001.
16. Hutchings, I.M. *Tribology: Friction and Wear of Engineering Materials*, 1st ed.; Butterworth Heinemann: Oxford, UK, 1992.
17. Bhushan, B. *Modern Tribology Handbook Principles of Tribology*, 3rd ed.; CRC Press LLC: Boca Raton, FL, USA, 2001; Volume 1, pp. 1094–1103.
18. Grice, N. An Experimental and Theoretical Study of Piston-Ring Lubrication. Ph.D. Thesis, Lancashire Polytechnic, Preston, UK, October 1990.
19. Garcia, A.F.G.; Smith, E.H.; Sherrington, I. Piston-ring film thickness: Theory and experiment compared. *Proc. I. Mech. E. Part. J J. Eng. Tribol.* **2018**, *232*, 550–567. [CrossRef]
20. Garcia, A.F.G.; Smith, E.H.; Sherrington, I. Mapping lubricating film thickness, film extent and ring twist for the compression-ring in a firing internal combustion engine. *Tribol. Int.* **2014**, *70*, 112–118. [CrossRef]

21. Shaw, M.C.; Nussorfer, T. A visual and photgraphic study of cylinder lubrication. *Natl. Advis. Comm. Aeronaut. (NACA) Rep.* **1947**, *850*, 247–266.
22. Saito, K.; Igashira, T.; Nakada, M. Analysis of oil consumption by observing behaviour around piston ring using a glass cylinder engine. *SAE Trans.* **1989**, *98*, 1027–1038.
23. Lee, P.M.; Priest, M.; Stark, M.; Taylor, R.I. The study of residence time and flow rate of lubricating oil through the top ring zone of a gasoline engine. *Proc. ASME ICES* **2009**, *43406*, 793–801.
24. Przesmitzki, S.; Tian, T. *Oil Transport Inside the Power Cylinder during Transient Load Changes*; SAE Paper: Warrendale, PA, USA, 2007.
25. Stark, M.S.; Gamble, R.J.; Hammond, C.; Gillespie, H.M.; Smith, J.R.; Nagatomi, E.; Priest, M.; Taylor, C.M.; Taylor, R.I.; Waddington, D.; et al. Measurement of lubricant flow in a gasoline engine. *Tribol. Lett.* **2005**, *19*, 163–168. [CrossRef]
26. Stark, M.S.; Wilkinson, J.J.; Lee, P.M.; Lindsay Smith, J.R.; Priest, M.; Taylor, R.I.; Chung, S. The degradation of lubricants in gasoline engines: Lubricant flow and degradation in the piston-assembly. In Proceedings of the 31st Leeds-Lyon Symposium on Tribology, Leeds, UK, 7–10 September 2004; Elsevier: San Diego, CA, USA, 2005; pp. 779–786.
27. Froelund, K.; Menezes, L.A.; Johnson, H.R.; Rein, O.R. *Real-Time Transient and Steady-State Measurement of Oil Consumption for Several Production SI-Engines*; SAE Paper: Warrendale, PA, USA, 2001. [CrossRef]
28. CIMAC Greenhouse Gas Strategy Group. Zero Carbon Energy Sources for Shipping. In *CIMAC Position Paper 2020*, 1st ed.; CIMAC: Frankfurt, Germany, 2020.